Multi-dimensional Spectroscopy of Polymer Films; Surface and Interfacial Interactions

Marek W. Urban

Department of Polymers and Coatings

North Dakota State University

Fargo, ND 58105, USA

SUMMARY: Behavior of macromolecules near surfaces and interfaces of polymeric thin films and coatings may play a vital role in numerous applications. Therefore, understanding of molecular level processes responsible for durability, adhesion, and many other macroscopic processes is of a particular importance. This presentation will focus on stratification processes in multi-component polymeric films, with particular emphasis to polymer-surfactant interactions in latexes, responsiveness of individual components during coalescence of water-borne polyurethanes, and behavior of thermoplastic olefins (TPO). The presence of macromolecular arrange-ments and interactions among various components near the film-air (F-A) and the film-substrate (F-S) interfaces can be effectively monitored using attenuated total reflectance (ATR) and step-scan photoacoustic (SS-PA) Fourier transform infrared (FT-IR) spectroscopy. Both approaches are capable of obtaining information from various surface depths and complement each other if one seeks molecular level information from 0 – 150 μm into the film. If one combines ATR and PA information with IR and/or Raman surface imaging, it is possible to obtain a 3-dimensional representation of polymeric films.

Introduction

Although there are numerous surface sensitive techniques utilized in polymer surface analysis, many require high vacuum operating conditions or sample preparation. As a result, the scope of analysis is often limited or obscured by altering a specimen. However, certain Fourier transform infrared (FT-IR) techniques[1] offer surface sensitivity and selectivity without vacuum limitations and broader range of applications. Such techniques, especially with current advances in FT-IR spectroscopy include internal reflection spectroscopy (IRS) techniques, such as attenuated total reflection (ATR)[2] as well as continuous-scan and step-scan photoacoustic (SS PAS), two-dimensional (2-D), and rheo-

 CCC 1022-1360/99/$ 17.50+.50/0

photoacoustic (RPA) measurements.[4-6] Significant advantages in quantitative analysis using ATR, enhanced sensitivity with step-scan photoacoustic FT-IR spectrometers, and the capability of IR/Raman surface imaging, make it possible to obtain 3-dimensional pictures of polymeric films. The following sections will provide a brief description of some recent advances in ATR, step-scan PA FT-IR, and FT-IR/Raman imaging as applied to analysis of surfaces and interfaces.

Attenuated Total Reflectance (ATR) Spectroscopy

Internal reflection spectroscopy (IRS) can be used to measure optical spectra of a sample in contact with an infrared transparent crystal of higher refractive index. As light passes through the crystal, a standing wave is formed at the sample-crystal interface. If the sample absorbs a portion of this radiation, the propagating wave is attenuated by the sample. This process is described as attenuated total reflectance (ATR) spectroscopy, which is a commonly used contact sampling method to obtain surface composition information from polymeric samples.[7,8] In the ATR procedure, as depicted in Figure 1, the infrared beam is directed at an incident angle (θ) through a crystal of refractive index n_1 onto a sample which is of lower refractive index n_2.

The passage of IR light through the ATR crystal depends on the critical angle (θ_c), which is defined as $\sin^{-1}n_2/n_1$. Due to the different refractive indices of the ATR crystal and sample, light reflects inside the crystal when $\theta > \theta_c$, and refracts out of the crystal for $\theta < \theta_c$, as illustrated in Figure 2. The internal reflection element and physical principles of ATR forms the basis of numerous configurations from which a wide variety of samples can be studied.[7]

One of the main advantages of IRS is that it is possible to conduct surface depth-profiling experiments by varying the angle of incidence and/or substituting ATR crystals with different refractive indices. The penetration depth, d_p, is expressed by the following equation:[2,7,9]

$$d_p = \frac{\lambda}{2\pi n_1 \left(\sin^2\theta - n^2_{21}\right)^{1/2}} \qquad (1)$$

where: d_p (μm) is the depth penetration into the surface; n_{21} is the refractive index ratio of the sample and crystal; and λ (μm) is the wavelength of electromagnetic

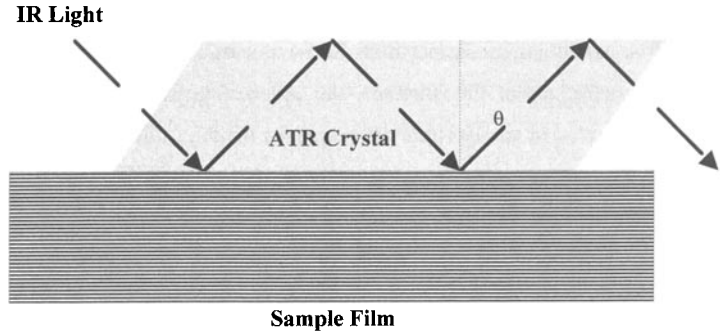

Figure 1. Schematic diagram of an ATR experiment.

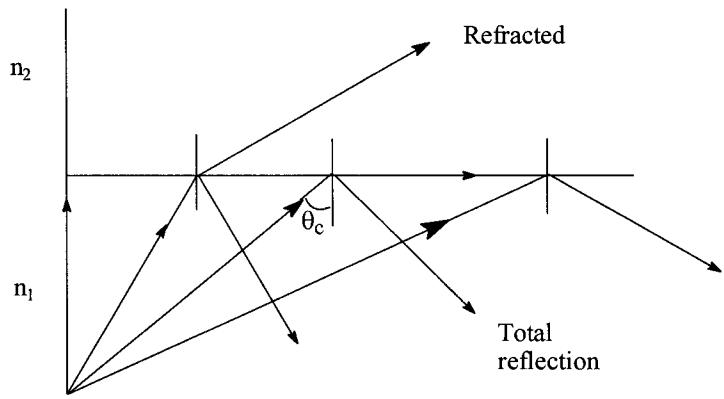

Figure 2. Schematic diagram of the effect of refractive index changes on the light path as a function of incidence angle.

radiation. Typical values for d_p are between 0.2 and 4 μm. Based on the surface depth profiling concept, ATR has been applied to numerous systems in the determination of stratification of components in organic coatings, including melamine-polyester,[10] alkyds,[11] urethanes,[12-14] and latexes.[16-26]

The surface sensitivity of ATR has proven to be quite useful for quantitative understanding of polymer substrates.[27,28] The determination of concentrations at specific

depths typically involves a quite complex approach, but is initially based on the calculation of an extinction coefficient from Beer-Lambert's law. As a means to quantify component concentrations at the interface, the absorbance index and reflective index spectra are incorporated in an algorithm developed for depth profiling, as shown in Figure 3.[2]

According to Eqn. (1), the penetration depth depends upon the wavelength of electromagnetic radiation and the angle of incidence. Since Eqn. (1) assumes homogeneous substrates, depth-profiling experiments are excluded from using this relationship for compositional stratification of the substrate. In order to adapt this relationship to quantitative analysis of nonhomogeneous surfaces, an algorithm was developed to overcome this problem.[29] In effect, a nonhomogeneous surface is numerically sliced to form a stack of parallel, thin homogeneous films, as illustrated in Figure 4. The surface is divided into n layers each with a layer thickness, h_j. At the each boundary layer, L_j, the response of the sample to local evanescent waves can be characterized by a complex refractive index defined by $\hat{n}_j = n_j - i\kappa_j$, where κ_j is referred to as the absorption index.[29] Applying this algorithm to each layer, one can obtain information from each layer which is assumed to be homogeneous. This approach facilitates the use of Eqn. (1) to each layer, but the layers among themselves are not homogeneous. Using the approach of stacking all layers together, the surface is reconstructed by a stepwise treatment of the volumes occupied by each layer. This approach allows accurate quantitative analysis of surfaces, and precision is determined by the number of spectra recorded at various depths.

Photoacoustic (PA) Fourier Transform Spectroscopy

Unlike ATR, photoacoustic spectroscopy is based on the direct detection of the energy absorbed by the sample and does not require contact with an optical element. As a result, this technique provides a means of analysis for opaque specimens of essentially any shape or morphology in a non-destructive manner.[3,30,31] The photoacoustic effect is a result of absorption of modulated radiation, producing corresponding temperature fluctuations at the sample surface. The coupling gas phase above the sample surface will undergo modulated pressure changes, producing a periodic acoustic signal. This acoustic response

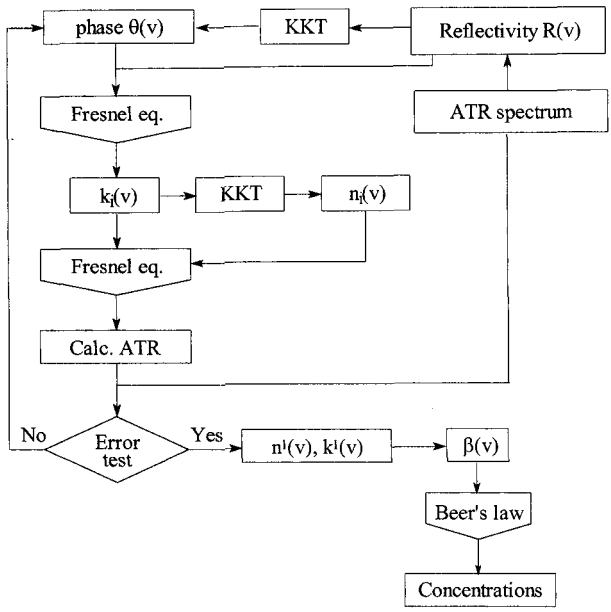

Figure 3. A schematic diagram of the algorithm for quantitative surface depth profiling.

is measured with a sensitive microphone, and the obtained electrical signal is Fourier-transformed, giving the PA spectra. Figure 5 illustrates this photoacoustic process. The basis of PA spectroscopy depends on the two-step process of radiation absorption and thermal diffusion. The amount of IR energy absorbed corresponds to the distribution of IR active functional groups throughout the specimen. The process of energy conversion to heat is fast (nanoseconds), so absorbed energy is immediately released as heat, which is transferred to the sample surface. The physics of this process has been mathematically detailed by Rosencwaig, in which the absorbed IR energy is represented by a thermal

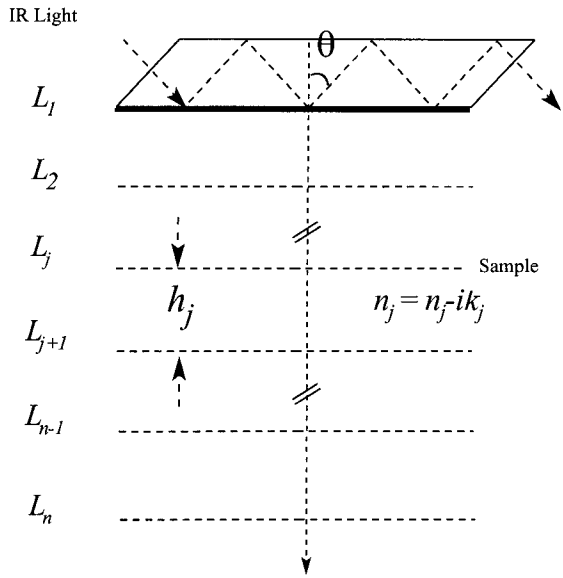

Figure 4. Schematic diagram of numerically slicing a nonhomogeneous surface to form a stack of parallel homogeneous layers.

signal defined by periodic boundary conditions which exponentially decreases as it approaches the surface.[31] Due to the dissipative transfer of thermal energy through the solid and gas phases, the concept of thermal diffusion length (μ_{th}) is introduced.[32] Over the distance μ_{th}, the thermal signal is attenuated by e^{-1} of the initial value, which is also the distance corresponding to 2π/modulation frequency ($2\pi/\omega$). Therefore, the PA spectra represents the IR functionalities from the surface to a depth of μ_{th} into the solid, and any response below μ_{th} will be lost. This relationship is represented as:

$$\mu_{th} = \left(\frac{2\alpha}{\omega}\right)^{1/2} \qquad (2)$$

where: α (cm^2/s) is the thermal diffusivity.[33]

Since the intensity of the optical or thermal signal decreases with distance, the photothermal response is dependent on sample thickness (ℓ), optical absorption length (ℓ_β), as well as μ_{th}.[32,] These factors allow surface depth profiling experiments, since by

altering the modulation frequency, μ_{th} will change, thus providing a different depth of penetration which may range from 0 to 150 μm. While PA FT-IR depth profiling experiments are very useful in surface and interfacial polymer analysis,[35-37] studies of polymer stratification and degradation,[38,39] time-dependent processes,[40-42] and polymer film formation[12,13,43,44] make the scope of this method even more versatile.

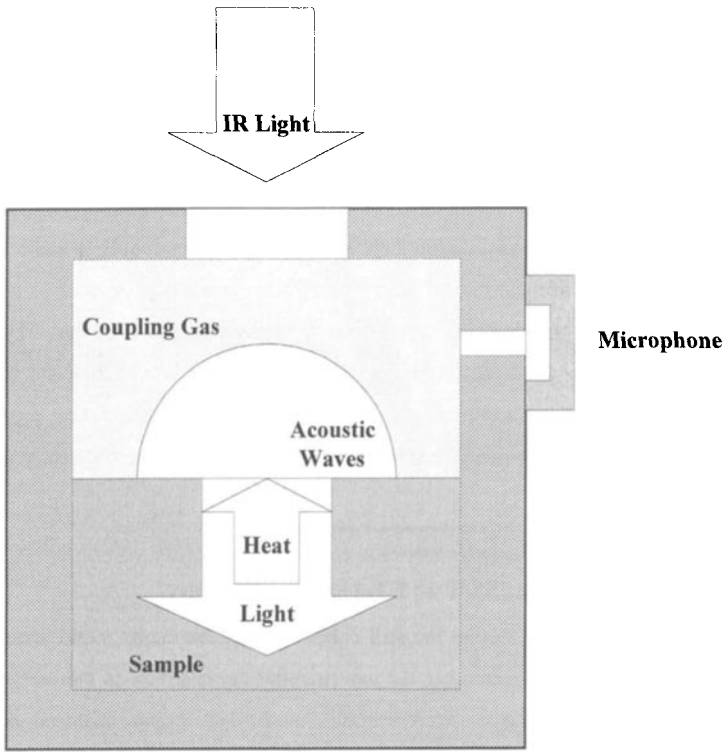

Figure 5. Schematic diagram of photoacoustic cell and generation of photoacoustic signal.

Over the last 20 years most of the PA FT-IR measurements have been with spectrometers operating in the continuous or rapid scan mode, in which the interferometer mirror moves at a constant velocity. The constantly changing optical retardation interferometrically modulates the intensity of each wavelength of the IR beam at a specific

Fourier modulation frequency, ω. By changing the interferometer mirror velocity (V; cm/s), surface depth profiling is achieved by altering in the modulation frequency of the infrared radiation.[47,45] This relationship is shown by the following equation:

$$\omega = 2\bar{\nu}V \qquad (3)$$

where: $\bar{\nu}$ is the spectral wavenumber in cm^{-1} units.[46,47]

Since PA measurements indirectly measure the time lag of the thermal signal to reach the surface, the introduction of phase analysis is useful in determining the depth localization of absorbing species in the specimen surface. Bertrand applied phase analysis to photoacoustic detection by the analysis of sorbed water at the surface of polyethylene.[48] These studies showed that the depth resolution using phase analysis was much higher than could be obtained by changing the modulation frequency. By implementing phase analysis of the photoacoustic signal, distinction between the surface and bulk signals can be improved by two orders of magnitude. One of the drawbacks of these, as well as previous studies, is the fact that the depth of penetration is wavenumber dependent. Thus, low wavenumber regions provide spectral information from deeper depths than for the high wavenumber. To eliminate this dependence and obtain a constant penetration depth over the entire spectral range, step-scan photoacoustic (SS-PA) FT-IR spectroscopy may be used.

Step-Scan Photoacoustic (SS-PA) FT-IR Spectroscopy

Although the majority of PA studies are still conducted in continuous, rapid scan mode, the use of step-scan analysis overcomes the wavenumber dependence. In step-scan mode, the interferometer mirror moves incrementally, with data being acquired at each retardation point. This results in elimination of the Fourier modulation frequency dependence. Therefore, step-scan PA FT-IR allows measurements at constant sampling depths, because a single modulation frequency is applied over the entire spectral range. Furthermore, precise timing of the signal collection and mirror position permits collection of in-phase (or I; in-phase with the incoming signal) and in-quadrature (Q; or 90° out-of-phase with the incoming signal) components of the photoacoustic signal.

Current methods of detection in step-scan require a modulated signal to achieve optimal response, therefore, the IR light must be altered by either amplitude-modulation (AM) or phase-modulation (PM). In amplitude-modulation, the IR beam is chopped to

produce a modulated PA signal.[33,49] AM techniques are seldom used, since the S/N ratio decreases by 50% as a result of the beam being partially blocked by the chopping device, producing a signal with a large DC component. In the PM mode, such as shown in Figure6, modulation results from dithering the mirror at each retardation during data collection, which modulates the IR beam as a result of constructive and destructive interference of the recombined beam passing through the interferometer.

The major advantage of PM over AM techniques in step-scan PAS FT-IR spectroscopy, is a higher source throughput, since the light is not blocked and PM digital signal processor (DSP) electronics can be used to select the proper modulation frequency. Thus, PM step-scan spectroscopy provides a constant modulation frequency for all wave-

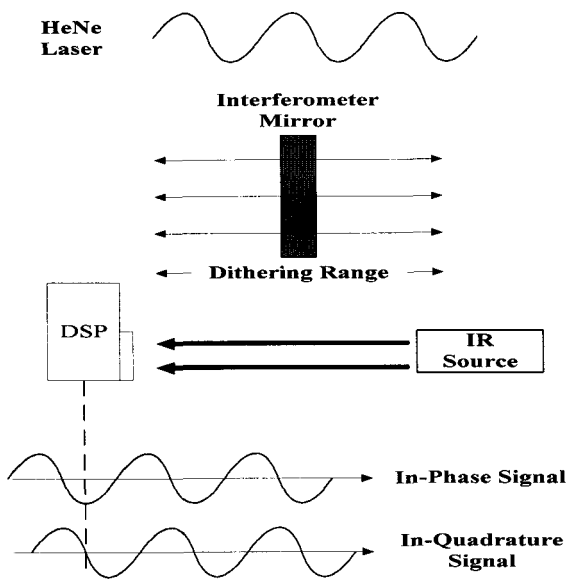

Figure 6. Schematic diagram of phase-modulation step-scan.

lengths and allows phase sensitive detection, providing precise control of the probe depth and convenient extraction of the signal phase.[50,51]

Significant advances have been made in recent years, because of the benefits of step-scan over conventional rapid-scan. Palmer et al. indicated that by changing the modulation frequency, depth information of plasma deposited films of cobalt

tetraphenylporphyrin and hexamethyldisilazane on the polypropylene can be obtained.[52,54] Furthermore, the combination of modulation frequency and phase analysis can be utilized to distinguish multiple layers. Bertrand demonstrated the optical absorption coefficient, β, of polymeric materials can be measured from the phase analysis.[48] Applying basic phase relationships to PA analysis allows separation of the surface and bulk signals. Poulet et al.[53] have shown that the photoacoustic phase (Ψ) for a homogeneous, thermally thick sample can be represented as a function of β and μ_{th} by:

$$\Psi = -\pi + \tan^{-1}(\beta\mu_{th} + 1) \qquad (4)$$

Since μ_{th} is held constant in step-scan, β can be obtained. Improvements to depth profiling resolution of ≤ 1 μm may be realized from utilization of the PA phase spectra.[54,55]

More applications of step-scan FT-IR spectroscopy open up through use of two-dimensional infrared (2-D IR) correlation spectroscopy.[6,56,57] In a typical 2-D correlation experiment, an external perturbation is applied to the system while changes of a spectroscopic response are recorded as spectral fluctuations.[58] By applying correlation analysis to signal fluctuations a 2-D plot can be generated, which shows spectral features generally not observable in 1-D analysis. Using this approach, one can take advantage of the extreme sensitivity of vibrational bands to changes in the local environment of functional groups. As indicated by previous 2-D FT-IR studies,[42-46] a wavenumber correlation map allows interpretation of vibrational coupling between specific functional groups and improved spectral resolution.

Surface Depth Profiling

One of the factors that may significantly influence surface composition of a substrate in the direction normal to the surface is stratification processes of individual components. This issue is particularly important for multi-component systems, such as thermoplastic olefin (TPO), since individual components may stratify at different rates and their concentration levels may vary as a function of distance from the surface. Figure 7 illustrates a series of SS-PA FT-IR spectra recorded at modulation frequencies of 1.9 $\bar{\nu}$ to 0.032 $\bar{\nu}$ over the range 1500 to 600 cm^{-1}. These allow surface depth profiling of deep regions below the surface, from approximately 4 to 50 μm. Integration of the band at 843 cm^{-1} due to crystalline PP phase shows the largest photoacoustic response at 7-9 μm below

the surface from the spectra recorded as Traces B, C, and D. Below 9 μm, this band gradually diminishes while going into the bulk. The EPR elastomer band at 720 cm^{-1} increases at the modulation frequency of 230 Hz. This spectral response indicates an increase of the CH rocking vibrational modes of ethylene units in EPR at an approximate penetration depth of 15 μm. These observations agree with the previous studies which showed that injection molding of EPR/PP blends will result in stratifying of the rubbery region below the surface.[64] However, the spectroscopic analysis presented here extends the scope of previous findings indicating that concentrations of PP and EPR components of TPO vary between 5 and 15 μm, with the EPR layer lying below the PP region.

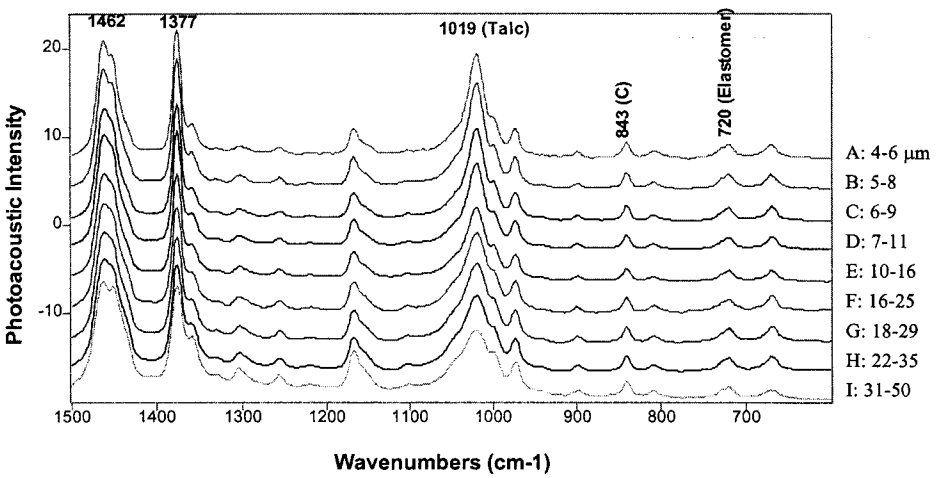

Figure 7. SS PA FT-IR spectra recorded from various depths from thermoplastic olefin (TPO).

Physico-chemical changes at the interface between two polymer surfaces have a significant effect on adhesion and molecular level processes associated with it. Although rheo-photoacoustic (RPA)[65,66] Fourier transform infrared (FT-IR) spectroscopy was developed to establish the origin of polymer-polymer interfacial interactions, no correlations were made between the spectroscopic data and the work of adhesion. The relationship between the vibrational energy changes in the C-H stretching region in polyethylene, induced by the interfacial stresses resulting from elongations of the substrate/coating double layer system, with the work of adhesion can be made. RPA FT-

IR spectra of the ACR/PE bilayer system at various elongations are illustrated in Figure 8, Traces A-E. It appears that the spectral features at 0% elongation (Trace A) are mainly due to the top layer, which is demonstrated by the presence of the CH_3 asymmetric and symmetric stretching bands at 2958 cm^{-1} and 2897 cm^{-1} due to the ACR top layer. As the specimen is elongated, the increase of the 2850 and 2930 cm^{-1} bands due to the methylene symmetric and asymmetric stretching of polyethylene are detected in Traces C-D, and the appearance of the substrate bands becomes more prominent. Furthermore, there is a vibrational energy shift of the substrate bands. At 0% elongation (Trace A), the symmetric C-H methylene stretching band due to polyethylene is detected at 2860 cm^{-1}, and as elongation progresses to 6% (Trace E), this band shifts to 2850 cm^{-1}.

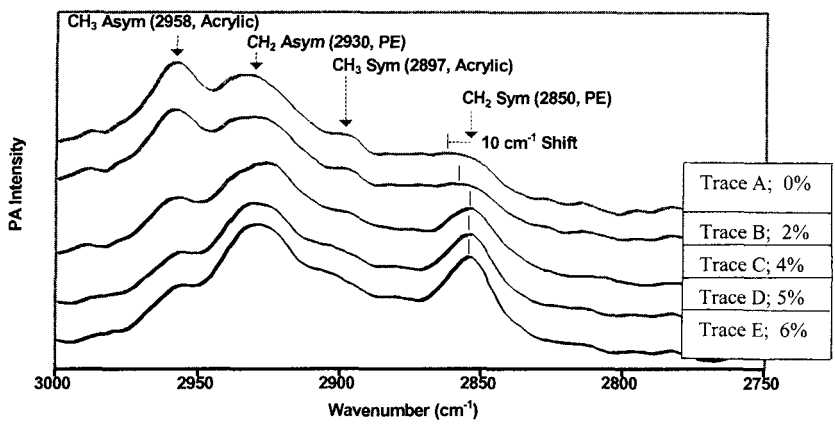

Figure 8. Rheo-photoacoustic FT-IR spectra of ACR/PE bilayer from 3000 to 2750 cm^{-1}.

One of the issues that is of great importance is understanding of molecular level processes leading to mobility of low molecular weight species to surfaces. In an attempt to determine SDOSS surfactant distribution during the film formation for a 50/50% styrene/n-butyl acrylate (p-Sty/p-nBA) latex copolymer and polymer blends several vibrational spectroscopic methods can be used. These ultimately lead to the development of 3-dimensional analysis of surfaces and depth profiling methodologies for latex films. Figure 9 shows FT-IR images obtained from the F-A and F-S interfaces of latex copolymer. As seen, aggregates are detected at the F-A interface, whereas the F-S interface appears to be uniform. In an effort to determine composition of aggregates at the

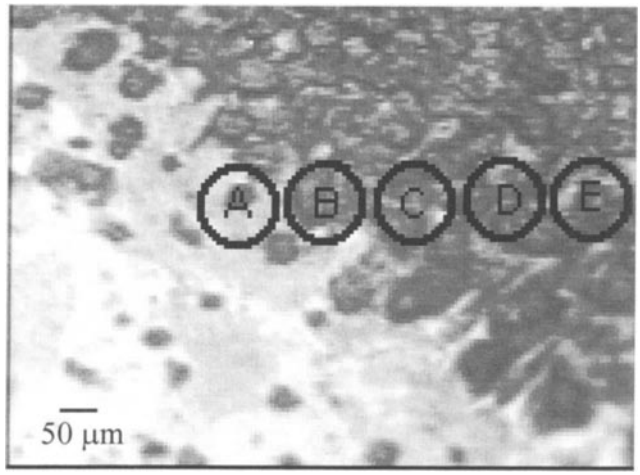

(a)

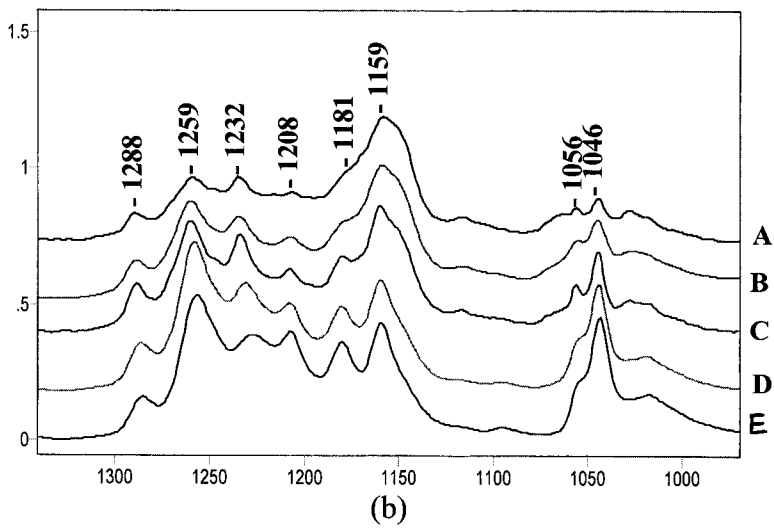

(b)

Figure 9. (a) FT-IR images of 50/50% Sty/n-BA latex copolymer recorded from the F-A interface points A, B, C, D, and E, and (b) their corresponding spectra.

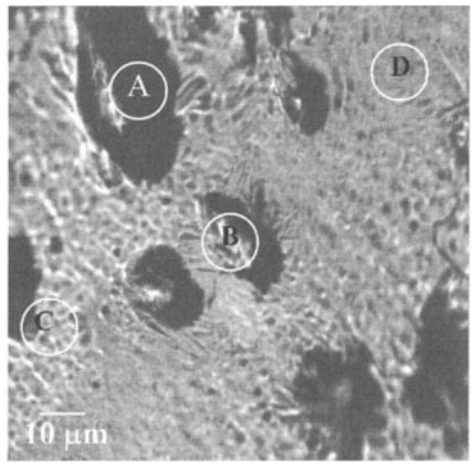

(a)

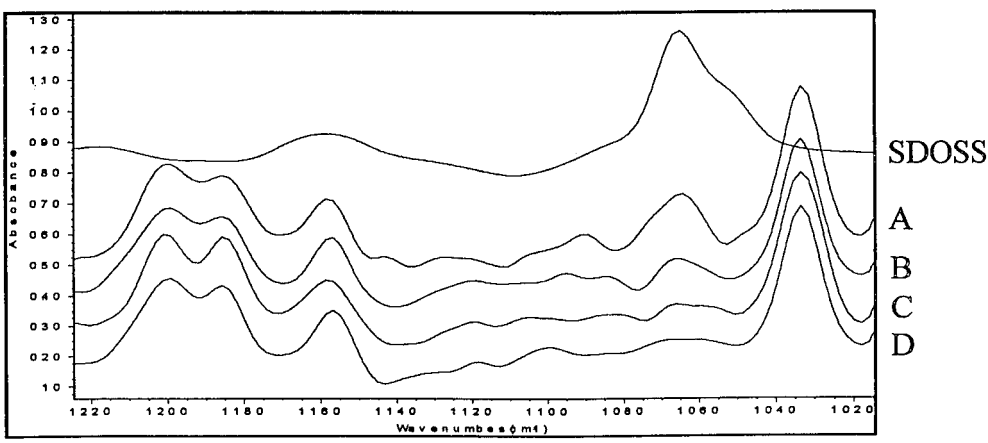

(b)

Figure 10. (a) FT-Raman images recorded from points: A, B, C, and, D, and (b) their corresponding spectra.

F-A interface, ATR microanalysis was performed. This is accomplished by focusing the IR beam and contacting ATR crystal with specimen diameter of 50 ~ 100 μm, and recording a spectrum from this area. While Figure 9 (a) shows circles from which the spectra were recorded at the F-A interface, Figure 9 (b) illustrates a series of spectra that correspond to points A, B, C, D, and E of Figure 9 (a). While the band at 1159 cm^{-1} due to C-O-C stretching mode of p-nBA holds constant, it appears that the intensities of the 1288, 1259, 1232, 1208, 1181, 1056, and 1046 cm^{-1} bands due to SDOSS surfactant increase while going from A to E. These results show that the observed aggregates shown in Figure 9 (a) are mainly composed of the SDOSS islands. Confirmation of the IR imaging studies can be seen in Figure 10, which illustrates FT-Raman spectra (Fig. 10 (b)) recorded from areas A, B, C and D indicated in Figure 10 (a). Again darker areas represent surfactant aggregates in the latex surface.

Summary

These studies show that a combination of FT-IR surface sensitive and selective techniques combined with surface imaging allows detection of numerous processes near the surfaces and interfaces of polymeric films. While quantitative surface depth profiling can be accomplished using ATR FT-IR spectroscopy, more advanced analysis that utilizes a photoacoustic affect is capable of phase rotational analysis from significantly greater depths. The utility of rheo-photoacoustic FT-IR allows detection of the work of adhesion. Processes leading to exudation of low molecular species to surfaces and interfaces can be effectively examined using FT-IR and FT-Raman imaging.

Acknowledgments

The author is thankful to the National Science Foundation I/U Research Center in Coatings at North Dakota State University and Eastern Michigan University for partial support of these studies.

References

1. Koenig, J. L. *Spectroscopy of Polymers*, American Chemistry Society, Washington, DC, 1992.
2. Urban, M. W. *Vibrational Spectroscopy of Molecules and Macromolecules on Surfaces,* Wiley-Interscience Publication, New York, 1993.
3. *Structure-Property Relationships in Polymers;* Urban, M.W.; Craver, C.D. Eds.; Am. Chem. Soc.: Washington, D.C., 1993.
4. Pennington, B.D.; Ryntz, R.A.; Urban, M.W. *Polym. Matl. Eng. Sci.*, **1997**, *77*, 591.
5. Pennington, B.D.; Urban, M.W. *Polym. Matl. Eng. Sci.*, **1996**, *75*, 39.
6. Noda, I.; Dowrey, A. E.; Marcott, C. *Appl. Spectrosc.* **1993**, *47*, 1317.
7. Harrick, N. J. *Internal Reflection Spectroscopy*, Interscience Publishers, New York, 1967.
8. Fahrenfort, J. *Spectrochim, Acta.* **1961**, *17*, 698.
9. Urban, M. W. *J. Adhes. Sci. Technol.* **1993**, *7*, 1.
10. Hirayama, T.; Urban, M.W., *Prog. Org. Coat.* **1992**, *20*, 81.
11. Salazar-Rojas, E.M.; Urban, M.W. *Prog. Org. Coat.* **1989**, *16*, 371.
12. Ludwig, B.W.; Urban, M.W. *J. Coat. Technol.* **1994**, *66*, 59.
13. Ludwig, B.W.; Urban, M.W. *J. Coat. Technol.* **1996**, *68*, 93.
14. Kaminski, A.M.; Urban, M.W. *J. Coat. Technol.* **1997**, *69*, 55.
15. Kaminski, A.M.; Urban, M.W. *J. Coat. Technol.* **1997**, *69*, 113.
16. Urban, M. W.; Evanson, K. W. *Polym. Commun.* **1990**, *31*, 279.
17. Evanson, K. W.; Urban, M. W. *J. Appl. Polym. Sci.* **1991**, *42*, 2287.
18. Evanson, K. W.; Urban M. W. *J. Appl. Polym. Sci.* **1991**, *42*, 2297.
19. Niu, B. J.; Urban, M. W. *J. Appl. Polym. Sci.* **1995**, *56*, 377.
20. Zhao, C. L.; Holl, Y.; Pith, T.; Lambla, M. *Coll. Polym. Sci.* **1987**, *265*, 823.
21. Thorstenson, T. A.; Evanson, K. W.; Urban, M. W. *Polym. Mater. Sci. Eng.* **1991**, *64*, 195.
22. Evanson, K. W.; Urban, M. W. *J. Appl. Polym. Sci.* **1991**, *42*, 2309.
23. Thorstenson, T. A.; Urban, M. W. *J. Appl. Polym. Sci.* **1993**, *47*, 1381.
24. Thorstenson, T. A.; Urban, M. W. *J. Appl. Polym. Sci.* **1993**, *47*, 1387.
25. Niu, B. J.; Urban, M. W. *J. Appl. Polym. Sci.* **1996**, *60*, 389.
26. Niu, B. J.; Urban, M. W. *J. Appl. Polym. Sci.* **1996**, *62*, 1903.
27. Carlsson, D.J.; Wiles, D.M. *Macromolecules* **1972**, *4*, 173.
28. Webb, J.R. *J. Polym. Sci.; Poly. Chem. Ed.* **1972**, *10*, 2335.
29. Huang, J.B.; Urban, M.W. *Appl. Spectrosc.* **1993**, *47*, 973.
30. Rosencwaig, A. *J. Appl. Phys.* **1978**, *49*, 2905.
31. Rosencwaig, A. *Photoacoustics and Photoacoustic Spectroscopy*, J. Wiley: New York, 1980.
32. Rosencwaig, A.; Gersho, A. *Science* **1975**, *190*, 556.
33. Rosencwaig, A. *Opt. Commun.* **1973**, *7*, 305.
34. Rosencwaig, A.; Gersho, A. J. *Appl. Phys.* **1976**, *47*, 64.
35. Urban, M. W. *J. Coat. Tech.* **1987**, *59*, 29.

36. Rosencwaig, A. *Ann. Rev. Biophys. Bioeng.* **1984**, *9*, 31.
37. Vidrine. D.W. *Appl. Spectrosc.* **1980**, *34*, 314.
38. Salazar-Rojas, E.M.; Urban, M.W. *J. Polym. Sci.: Poly. Chem.* **1990**, *28*, 1593.
39. Urban, M.W. *Prog. Org. Coat.* **1989**, *16*, 371.
40. Huang, J.B.; Urban, M.W. *J. Chem. Phys.*, **1993**, *98*, 5259.
41. Huang, J.B.; Urban, M.W. *J. Chem. Phys.*, **1994**, *100*, 4509.
42. Palmer, R.A.; Chao, J.L.; Dittmar, R.M.; Gregoriou, V.G.; Plunkett, S.E. *Appl. Spectrosc.* **1993**, *47*, 1297.
43. Urban, M.W.; Gaboury, S.R. *Macromolecules* **1989**, *22*, 1486.
44. Gaboury, S.R.; Urban, M.W. *ACS Proc. PMSE* **1989**, *60*, 875.
45. Chatzi, E.G.; Urban, M.W.; Ishida, H.; Koenig, J.L. *Polymer* **1986**, *27*, 1850.
46. *Transform Techniques in Chemistry*; Griffiths, P.R.; Plenum: New York, 1978, 122.
47. Griffiths, P.R.; DeHaseth, J.A. *Fourier Transform Infrared Spectrometry*; Chemical Analysis Series 83, Wiley: New York, 1986, 43.
48. Bertrand, L. *Appl. Spectrosc.* **1988**, *42*, 134.
49. Palmer, R. A. *Spectroscopy*, **1993**, *8*, 26.
50. Manning, C. J.; Dittmar, R. M.; Palmer, R. A.; Chao, L. J. *Infrared Phys.* **1992**, *33*, 53.
51. Dittmar, R. M.; Chao, J. L.; Palmer, R. A. *Appl. Spectrosc.* **1991**, *45*, 1104.
52. Gregoriou, V. G.; Daun, M. Schauer, M. W.; Chao, J., L.; Palmer, R. A. *Appl. Spectrosc.* **1993**, *47*, 1311.
53. Poulet, P; Chambron, J.; Unterreiner, R. *J. Appl. Phys.* **1980**, *51*, 1738.
54. Palmer, R.A.; Jiang, E.Y.; Chao, J.L. *Proc. SPIE* **1993**, *2089*, 250.
55. Palmer, R.A.; Jiang, E.Y. *Proceedings of the 8th International Topical Meeting on Photoacoustic and Photothermal Phenomena J. Phys. (Paris) IV, C and C7, Suppliment J. Phys.* **1994**, *4*, C7.
56. Noda, I. *Appl. Spectrosc.* **1993**, *47*, 1329.
57. Noda, I. *Appl. Spectrosc.* **1993**, *47*, 1337.
58. Noda, I. *J. Am. Chem. Soc.* **1989**, *111*, 8116.
59. Budevska, B.O.; Manning, C.J.; Griffiths, P.R.; Boginski, R.T. *Appl. Spectrosc.* **1993**, *47*, 1843.
60. Marcott, C.; Dowery, A.E.; Noda, I. *Appl. Spectrosc.* **1993**, *47*, 1324.
61. Gregoriou, V.G.; Noda, I.; Dowrey, A.E.; Marcott, C.; Chao, J.L.; Palmer, R.A. *J. Polym. Sci., Polym. Phys. Ed.* **1993**, *31*, 1769.
62. Jayarman, A. *Rev. Modern Phys.* **1983**, *55*, 65.
63. Weinstein, B.A.; Zallen, R. *Topics Appl. Phys.* **1984**, *54*, 463.
64. *Thermoplastic Elastomers from Rubber-Plastic Blends*; De, S.K.,Bhowmick, A.K., Eds.; Ellis Horwood: New York, 1990.
65. MacDonald, F; Goettler, H.; Urban, M.W. *Appl. Spectrosc.* **1989**, *43(8)*, 1387.
66. MacDonald, F.; Urban, M.W. *J. Adhesion Sci. Technol.* **1990**, *4(9)*, 751.